Carbon Monoxide Dissociation on Rh Nanopyramids

F. Buatier de Mongeot,[1] A. Toma,[1] A. Molle,[1] S. Lizzit,[2] L. Petaccia,[2] and A. Baraldi[3,4,*]

[1]*Dipartimento di Fisica, Università di Genova, Via Dodecaneso 33, 16146 Genova, Italy*
[2]*Sincrotrone Trieste S.C.p.A., S.S. 14 Km 163.5, 34012 Trieste, Italy*
[3]*Dipartimento di Fisica, Università degli Studi di Trieste and CENMAT, Via Valerio 2, 34127 Trieste, Italy*
[4]*Laboratorio TASC INFM-CNR, S.S. 14 Km 163.5, 34012 Trieste, Italy*

(Received 7 March 2006; published 3 August 2006)

CO dissociation on rhomboidal faceted nanopyramids, produced on Rh(110) by fine-tuning of ion irradiation conditions, has been studied by high resolution core-level spectroscopy. We find that this morphology presents a large efficiency towards CO dissociation, a process which is inhibited on flat (110) terraces. We also measured the reactivity of nanostructures bound by different artificial step distributions identifying the sites responsible for the molecular bond disruption in the undercoordinated ($n = 6$) edges running along the $[1\bar{1}2]$ equivalent directions, with CO sitting in on-top configuration.

DOI: 10.1103/PhysRevLett.97.056103 PACS numbers: 68.43.−h, 68.55.Jk, 82.45.Jn

The control of the atomic step distribution of clusters and nanostructures is of utmost importance in determining, among others, their magnetic [1], electrical, and catalytic properties. In this last context it was, for example, shown that the chemical reactivity of MoS_2 supported on gold surfaces is determined by the local electronic properties of the edge atoms, the basal plane of the molybdenum disulfide being inert for this reaction [2].

Recent experiments and theoretical models have tried to elucidate the atomistic details underlying the enhanced surface chemical reactivity of transition metals (TM). In particular, density functional theory (DFT) suggested that the *d*-band center shift and the relative change in the molecular-substrate interaction strength on low-coordinated atoms is the main reason for the barrier reduction in molecular dissociation [3–5].

In this respect, CO dissociation on TM stepped surfaces and supported clusters is particularly important in heterogeneous catalysis being one of the fundamental steps in the Fisher-Tropsch catalytic reaction, where carbon monoxide and hydrogen are converted into hydrocarbons [6,7]. For example, it has been found that Ru atomic step sites exhibit enhanced CO dissociation activity compared to smooth (001) terrace sites [8,9]. A strong size-dependent CO dissociation reactivity of nickel nanocluster deposited on oxide surfaces has been also demonstrated [10]. On Rh, previous results have shown that CO dissociation is negligible on close packed (111), (110), and (100) surfaces [11], and that it increases on stepped (211) [12] and (210) [13] Rh substrates. Experiments on Rh clusters supported on alumina surfaces have shown a strong size dependence of the reactivity towards CO dissociation [14,15], but the nature of the active sites was not explained.

Recently, it has been found that it is possible to tune the morphology and step distribution of a crystalline Rh(110) substrate by controlled exposure to a beam of noble gas ions: Xe ion irradiation at few hundreds eV leads to the formation of nonequilibrium periodic nanostructures such as nanoscale ripples, oriented either along [001] or $[1\bar{1}0]$ directions, mounds, and unexpected rhomboidal pyramids (RP) [16]. The latter nanostructures are particularly interesting as candidate model systems for testing catalytic reactivity, since they are endowed with steep facets running along nonequilibrium directions, exposing a high density of undercoordinated atoms.

In order to probe the reactivity of artificially prepared Rh nanostructures we used high-energy resolution x-ray photoelectron spectroscopy (XPS) at the SuperESCA beam line of ELETTRA [17] to monitor the CO adsorption sites, the dissociation process, and the formation of C and O atomic species. Our results show that on the Rh nanostructures CO dissociation takes place at temperatures as low as 350 K, and that about 10% of a CO saturated layer formed on the RP dissociate upon annealing to 560 K. The fraction of dissociated CO drastically increases with decreasing the initial CO coverage and reaches $\approx 80\%$ when the initial coverage is only 0.03 ML. The reason of such high efficiency is the high density of local atomic configurations with very low-coordinated Rh surface atoms ($n = 5$ and 6), with CO sitting in on-top configuration.

The growth of the RP nanostructures was characterized *in situ* by low energy electron diffraction (LEED). Figure 1(a) shows an out-of-phase electron diffraction pattern. The appearance of a fourfold splitting of the (00) diffraction peak along diagonal directions (inset) demonstrates the formation of the RP facets. The diffraction pattern is in agreement with the spot profile analysis (SPA)-LEED results reported in Ref. [16]. From the orientation of the splitted satellites, which form an angle of about 35° with respect to the $[1\bar{1}0]$ direction, we deduce that the surface is arranged in a close packing of faceted nanoscale pyramids which expose steps running along the four equivalent $[1\bar{1}2]$ directions.

The average facet slope, determined by the satellite splitting as a function of the vertical scattering phase S_z [Fig. 1(b)], turns out to be 12° corresponding to a step size

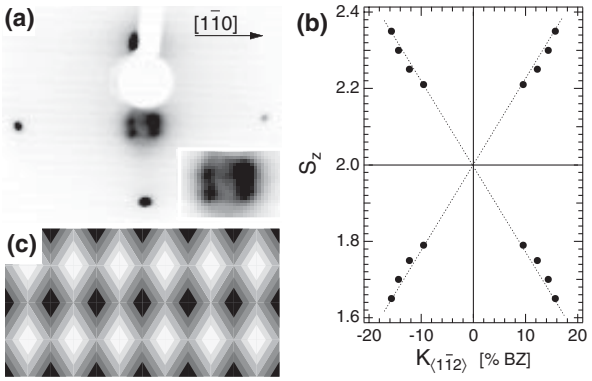

FIG. 1. (a) LEED pattern of the nanostructured Rh(110) substrate recorded at $E = 64$ eV showing diffraction satellites arising from the faceted rhomboidal pyramids (inset zoom of the (0, 0) diffraction peak enlarged 2.5 times). (b) Plot of the satellite splitting along $\langle 1\bar{1}2\rangle$ vs the vertical scattering phase S_z. (c) Real space model of RP nanostructures.

of about 3 lattice spacings. This is a large step density, which suggests that the reactivity should be correspondingly scaled up. The SPA-LEED data [16] reveal that the nanostructures are periodically ordered with a lateral correlation length of approximately 15 nm along the $\langle 100\rangle$ azimuth, leaving in between no extended flat (110) regions as confirmed by the disappearance of the (00) Bragg intensity in the inset of Fig. 1(a). In Fig. 1(c) we show a schematic pictorial view of the lateral arrangement of RP according to the present data and those of Ref. [16].

A cartoon model of the RP nanocrystals showing the geometry and the undercoordinated step sites is presented in Fig. 2 (left), where the number of exposed layers (and the lateral dimensions) have been scaled down by a factor 2.5. The morphology of the RP nanostructures is metastable, and tends to relax towards the flat fcc(110) morphology upon annealing. We verify that the morphology of the RP surface is preserved in the temperature range below 560 K where CO dissociation and desorption take place.

Once prepared, the RP were exposed to CO at $T =$ 200 K (1×10^{-8} mbar for 10 min) which corresponds to a saturated layer. C1s and O1s core-level spectra were

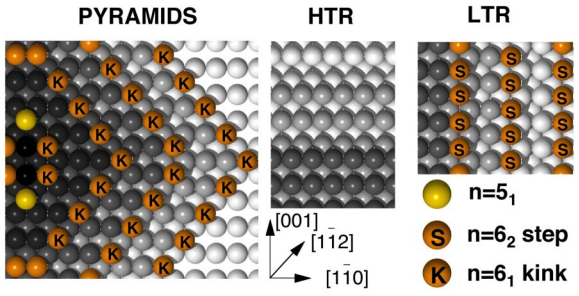

FIG. 2 (color online). Model for the RP determined in accordance with the LEED data and for the high temperature ripples and low temperature ripples phases.

measured at a photon energy of 400 eV and 650 eV, respectively, and at normal emission. The overall energy resolution was 150 meV ($h\nu = 400$ eV) and 300 meV ($h\nu = 650$ eV). Figure 3(a) (left) shows the evolution of the C1s spectra measured at 250 K after annealing of the saturated layer at different temperatures. The presence of two components at 286 and 285.55 eV reflects the occupation of two different adsorption sites. This result is confirmed by the O1s spectra (not reported) which show also two peaks at 531.7 and 530.9 eV. Thanks to the high sensitivity of XPS to the molecular adsorption site we can assign the higher C1s binding energy component to CO adsorbed in on-top sites, while the lower binding energy peak is related to CO chemisorbed in bridge sites, in agreement with previous XPS studies on Rh(110) [18,19]. Indeed, the increase of C1s binding energy while decreasing the coordination to the substrate is a general relationship, valid not only for Rh, but also for different TM surfaces, ranging from Ni to Pt [20]. Upon a temperature increase, the C1s spectra drastically change: the two components at 286 and 285.55 eV lose intensity due to CO desorption and slightly shift towards lower binding energies at higher temperatures [21].

However, the most important feature is the growth of a lower binding energy component at 283.55 eV, which is assigned, by comparison with previous experiments [14], to atomic carbon originating from dissociated CO. The evolution of the O1s spectra follows the same behavior indicating an increase of surface atomic oxygen (O1s peak at 528 eV). By fitting the C1s spectra with Doniach-Sunjic function [22] convoluted with Gaussians, we obtained the plot for the three different species [Fig. 3(a), right]. Up to about 350 K the CO coverage decrease is due only to desorption while at higher temperature even CO dissociation takes place. In agreement with experiments performed on flat Rh surfaces, on-top CO is the only species present on the surface above 450 K. With increasing the surface temperature the CO desorption or decomposition process is completed: a fraction of $9.4 \pm 0.5\%$ of the initial CO has converted into atomic carbon.

When a lower initial coverage is used the surface is mostly occupied by CO in on-top configuration. As shown in Fig. 3(b), we observe a similar temperature behavior of the surface population, with the population of bridge-bonded CO disappearing before the on-top species and the atomic carbon coverage increasing at temperatures above 370 K. Our data thus unambiguously show that when bridge-bonded CO is absent, atomic C still grows, as a product of dissociation of on-top CO. Now the fraction of dissociated CO at 560 K is much larger ($22 \pm 3\%$). The tendency to a higher dissociation probability for a lower initial coverage has been confirmed by the results obtained when a very low initial on-top coverage [$\Theta = 0.03$ ML, Fig. 3(c)] is present on the surface. In this case $80 \pm 14\%$ of the CO molecules undergoes dissociation.

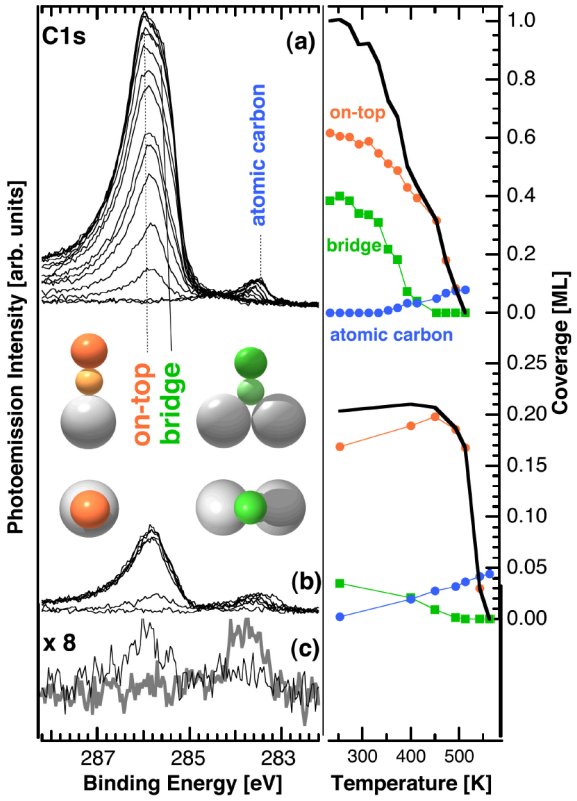

FIG. 3 (color online). (a) Left: sequence of C1s spectra for a saturated CO layer after annealing at increasing temperature and quenching to 250 K. Right: fitted area of the C1s peaks due to CO in on-top (red dots) and bridge (green squares) sites, due to total CO signal (full line) and to dissociated atomic carbon (blue dots). (b) Same as above for a lower initial CO dose ($\Theta =$ 0.21 ML). (c) C1s core-level spectra for a very low CO initial dose $\Theta = 0.03$ ML (black trace) and after annealing to 570 K (gray trace).

The broad choice of artificial configurations of atomic steps that can be obtained by varying preparation conditions allowed us to probe the CO reactivity for different nanostructures. In particular, we prepared ripples running along $[1\bar{1}0]$ (high temperature ripples, HTR) and along [001] (low temperature ripples, LTR), both structures endowed with a high density of steps. The local structure of these two phases is reported in Fig. 2. Photoemission results indicate that for HTR and LTR $\approx$4% of the saturated CO layer undergoes dissociation, while for the flat Rh(110) the reactivity for CO dissociation is just 2.4%. The residual carbon revealed upon annealing of the flat Rh(110) is likely originated on steps, which represents, even for a very well prepared surface with a miscut of 0.2°, $\approx$1% of the population.

At variance with the (111), (100), and (110) flat Rh surfaces which present first layer atoms with 9, 8, and 7 coordination, respectively, the RP, see Fig. 2, are composed by a large number of five and sixfold coordinated atoms. We associate the high reactivity of Rh nanopyramids towards CO dissociation with the presence of these undercoordinated Rh atoms, with CO molecules occupying preferentially on-top configurations. The lower is the metal coordination number n of the surface atoms, the smaller the Rh d bandwidth that results in a shift of the d-band center towards lower binding energy. The higher reactivity of these low-coordinated TM atoms towards molecular dissociation has been proven for a large number of systems [8,9,23,24].

In Table I we have estimated the density of local atomic configurations for the different morphologies that we have produced. The typical average dimension of the RP clusters are 15 nm along the $[1\bar{1}0]$ direction, i.e., 2.5 times larger than shown in the model of Fig. 2, corresponding to an average number of 12 exposed layers. The data have been reported according to the number n_l of nearest (n) and next-nearest (l) neighbors. What appears peculiar to the RP, with respect to the LTR and HTR morphology, is the very high density of kinked microfacets, produced by the steps running along $[1\bar{1}2]$, which provide a high density of low-coordinated atoms labeled K in Fig. 2. The local atomic configuration of the RP microfacets represents an *open* morphology [the nearest neighbor (n.n.) number is 6 with only 1 next n.n.], with an increase of $\approx$73% of the distance between Rh atoms along the steps compared to the nearest neighbor distance of bulk Rh. Indeed, with decreasing the initial CO coverage the availability of 6_1 Rh atoms, with CO sitting in on-top sites (estimated surface densities between 3% and 34%, respectively), increases, thus result-

TABLE I. Relative percent occupancy of the various surface sites enumerated n_l according to the number of nearest n and next-nearest l neighbors for the different nanostructures (RP, HTR, and LTR) and for the singular (110) terrace. The sites enumerated according to their coordination number can be identified in the following way: 5_1 = upper step corner atom, 6_1 = upper step (100) facet, 7_1 = upper step (111) facet, 7_2 = (110) terrace atoms, 8_1 = lower step RP facets, 9_2 = lower step (111) facets, 9_2 = lower step (100) facets.

Site	5_1	6_1	6_2	7_1	7_2	8_1	$9_{2-(111)}$	$9_{2-(100)}$
RP	2.8	33.9			35.8	23.9	1.8	1.8
HTR				33	33			33
LTR			33		33			33
Terrace					100			

ing in a higher fraction of dissociated CO. We expect that the activation energy for CO dissociation on these sites can be even lower than on the Rh(211) steps ($n = 7$) or kinks ($n = 6$) for which calculations [25] have found activation energies of 0.30 and 0.21 eV, respectively.

As for Ru(109) [8,9], CO preferentially dissociates on RP when placed in on-top configuration. This is at variance with the case of Rh clusters supported on alumina [14], where the bridge site was suggested to be the favorite initial state. This difference can be explained with the higher energetic stability of on-top CO on sixfold coordinated Rh atoms on the RP. Indeed, the on-top site has been proven to be the favorite adsorption configuration at low coverage on a large number of flat [26] and stepped Rh surfaces [24]. However, as pointed out by Liu *et al.* [25], not only adsorption sites and atomic coordination, but even geometrical effects involved in the transition state complex, can contribute to the magnitude of the dissociation barrier. Detailed modeling of the electronic configuration in those sites is needed to determine the modification of the projected density of states onto the 4*d* orbitals for the low-coordinated atoms.

If we consider the experiments about CO dissociation on alumina supported Rh clusters [14], we observe that a maximum in the dissociation fraction of 50% was found for clusters of around 1100 atoms, while the reactivity suddenly decreased to 30% for bigger clusters. Though in that work no structural information relative to the shape of the clusters was provided, we can very reasonably expect that for relatively small clusters, the relative density of low-coordinated atoms, similar to the RP kinked edges along the ridges of the clusters, becomes important. The RP clusters produced in the present experiment turn out to be formed on average by about 3200 Rh atoms, and have a reactivity comprised between 80% and 10% depending on the initial CO coverage, which compares well with the 30% reactivity of the clusters of corresponding size, suggesting that the role of the alumina support is marginal and that edge effects should be dominant.

In conclusion, we have shown that artificially prepared Rh nanopyramids can induce the dissociation of CO, which would otherwise desorb intact on the (110) terraces. A comparison of different nanostructures allows to indicate that the most probable reaction site for CO dissociation is an on-top configuration at the kinked step edges where Rh atoms have the lowest coordination. Core-level photoelectron spectroscopy data indicate that at high CO coverage the dissociation is almost 10% and increases with decreasing the initial CO coverage up to 80%, which compares well with the data for alumina supported clusters of comparable size. The possibility to form nanostructured surfaces with high density of low-coordinated atoms opens up the possibility to artificially increase the surface reactivity in a controlled way.

We thank U. Valbusa for useful discussion and insightful suggestions, and acknowledge financial support from the MIUR under the Programs No. PRIN2003, No. FIRB2001, and from Fondazione CARIGE.

*Corresponding author.
Email address: alessandro.baraldi@elettra.trieste.it

[1] R. Moroni *et al.*, Phys. Rev. Lett. **91**, 167207 (2003).
[2] S. Helveg *et al.*, Phys. Rev. Lett. **84**, 951 (2000).
[3] B. Hammer and J. K. Nørskov, Surf. Sci. **343**, 211 (1995).
[4] B. Hammer, O. H. Nielsen, and J. K. Nørskov, Catal. Lett. **46**, 31 (1997).
[5] S. Dahl *et al.*, Phys. Rev. Lett. **83**, 1814 (1999).
[6] Y. Zhang, G. Jacobs, D. E. Sparks, M. E. Dry, and B. H. Davis, Catal Today **71**, 411 (2002).
[7] G. A. Somorjai, *Introduction to Surface Chemistry and Catalysis* (Wiley, New York, 1994).
[8] T. Zubkov, G. A. Morgan, Jr., and J. T. Yates, Jr., Chem. Phys. Lett. **362**, 181 (2002).
[9] T. Zubkov *et al.*, Surf. Sci. **526**, 57 (2003).
[10] U. Heiz, F. Vanolli, A. Sanchez, and W. D. Schneider, J. Am. Chem. Soc. **120**, 9668 (1998).
[11] J. C. Campuzano, in *The Chemical Physics of Solid Surfaces and Heterogeneous Catalysis*, edited by D. A. King and D. P. Woodruff (Elsevier, New York1990), Vol. 3, p. 389.
[12] M. Mavrikakis, M. Baumer, H.-J. Freund, and J. K. Nørskov, Catal. Lett. **81**, 153 (2002).
[13] M. Rebholz, R. Prins, and N. Kruse, Surf. Sci. **259**, L797 (1991).
[14] S. Andersson *et al.*, J. Chem. Phys. **108**, 2967 (1998).
[15] G. Ertl and H.-J. Freund, Phys. Today **52**, No. 1, 32 (1999).
[16] A. Molle *et al.*, Phys. Rev. Lett. **93**, 256103 (2004).
[17] A. Baraldi *et al.*, J. Electron Spectrosc. Relat. Phenom. **76**, 145 (1995).
[18] A. Baraldi *et al.*, Surf. Sci. Rep. **49**, 169 (2003).
[19] A. Baraldi *et al.*, Surf. Sci. **367**, L67 (1996).
[20] N. Martensson and A. Nilsson, in *Springer Series in Surface Science*, edited by W. Eberhardt (Springer-Verlag, Berlin, 1994), Vol. 35.
[21] This is due to changes of intermolecular interactions between CO molecules in on-top sites or partial occupation of threefold sites on the (111) facets of the RP.
[22] S. Doniach and M. Sunjic, J. Phys. C **3**, 285 (1970).
[23] B. Hammer and J. K. Nørskov, Adv. Catal. **45**, 71 (2000).
[24] M. Mavrikakis, B. Hammer, and J. K. Nørskov, Phys. Rev. Lett. **81**, 2819 (1998).
[25] Zhi-Pan Liu and P. Hu, J. Am. Chem. Soc. **125**, 1958 (2003).
[26] H. Over, Prog. Surf. Sci. **58**, 249 (1998).